



This is a repository copy of *Temporal variations in the potential hydrological performance of extensive green roof systems*.

White Rose Research Online URL for this paper:
<http://eprints.whiterose.ac.uk/127701/>

Version: Accepted Version

Article:

De-Ville, S., Menon, M. orcid.org/0000-0001-5665-7464 and Stovin, V. orcid.org/0000-0001-9444-5251 (2018) Temporal variations in the potential hydrological performance of extensive green roof systems. *Journal of Hydrology*, 558. pp. 564-578. ISSN 0022-1694

<https://doi.org/10.1016/j.jhydrol.2018.01.055>

Reuse

This article is distributed under the terms of the Creative Commons Attribution-NonCommercial-NoDerivs (CC BY-NC-ND) licence. This licence only allows you to download this work and share it with others as long as you credit the authors, but you can't change the article in any way or use it commercially. More information and the full terms of the licence here: <https://creativecommons.org/licenses/>

Takedown

If you consider content in White Rose Research Online to be in breach of UK law, please notify us by emailing eprints@whiterose.ac.uk including the URL of the record and the reason for the withdrawal request.



eprints@whiterose.ac.uk
<https://eprints.whiterose.ac.uk/>

Temporal variations in the potential hydrological performance of extensive green roof systems

Simon De-Ville^{a,*}, Manoj Menon^b, Virginia Stovin^c

^a*School of Architecture, Building & Civil Engineering, Loughborough University, Loughborough, LE11 3TU, UK*

^b*Department of Geography, University of Sheffield, Sheffield, S10 2TN, UK*

^c*Department of Civil & Structural Engineering, University of Sheffield, Sir Frederick Mappin Building, Mappin Street, Sheffield, S1 3JD, UK*

Abstract

Existing literature provides contradictory information about variation in potential green roof hydrological performance over time. This study has evaluated a long-term hydrological monitoring record from a series of extensive green roof test beds to identify long-term evolutions and sub-annual (seasonal) variations in potential hydrological performance. Monitoring of nine differently-configured extensive green roof test beds took place over a period of 6 years in Sheffield, UK.

Long-term evolutions and sub-annual trends in maximum potential retention performance were identified through physical monitoring of substrate field capacity over time. An independent evaluation of temporal variations in detention performance was undertaken through the fitting of reservoir-routing model parameters. Aggregation of the resulting retention and detention variations permitted the prediction of extensive green roof hydrological

*Corresponding author

Email address: s.de-ville@lboro.ac.uk (Simon De-Ville)

performance in response to a 1-in-30-year 1-hour summer design storm for Sheffield, UK, which facilitated the comparison of multi and sub-annual hydrological performance variations.

Sub-annual (seasonal) variation was found to be significantly greater than long-term evolution. Potential retention performance increased by up to 12% after 5-years, whilst the maximum sub-annual variation in potential retention was 27%. For vegetated roof configurations, a 4% long-term improvement was observed for detention performance, compared to a maximum 63% sub-annual variation. Consistent long-term reductions in detention performance were observed in unvegetated roof configurations, with a non-standard expanded-clay substrate experiencing a 45% reduction in peak attenuation over 5-years. Conventional roof configurations exhibit stable long-term hydrological performance, but are nonetheless subject to sub-annual variation.

Keywords: Green Roof, Seasonal, Annual, Retention, Detention, Hydrological Performance

1 **Highlights**

- 2 • Temporal changes in potential performance evaluated over 6 years for
3 9 test beds
- 4 • Potential retention performance identified via monitored field capacity
- 5 • Detention performance explored via the fitting of simple hydrological
6 models
- 7 • Long-term performance evolutions are small in traditional green roof
8 configurations

- 9 • Sub-annual (seasonal) variations are dominant over long-term evolu-
10 tions

11 **1. Introduction**

12 *1.1. Background*

13 It has been widely demonstrated that extensive green roof systems offer
14 stormwater management capabilities through two hydrological processes, the
15 retention of rainfall (which subsequently is lost via evapotranspiration and
16 does not become runoff), and the detention of runoff (the transient storage of
17 rainfall as it passes through the roof layers). Stormwater managers typically
18 assume that a green roof’s physical characteristics — such as its hydraulic
19 conductivity (which influences detention) and field capacity (which influences
20 retention) — are constant over time, and therefore that the roof’s potential
21 to retain and detain runoff are also constant over time. However, these prop-
22 erties may change in response to seasonal factors (vegetation growth cycles,
23 substrate wetting/drying regimes) and/or due to longer-term processes such
24 as compaction (De-Ville et al., 2017). There is therefore a need to deter-
25 mine whether there is evidence of such seasonal or longer-term changes in
26 the underlying potential performance characteristics.

27 The most frequently reported indicator of green roof hydrological per-
28 formance is the percentage retention, reported as either a ‘mean per-event’
29 or ‘total volumetric’ retention. Many green roof monitoring programmes
30 have highlighted seasonal trends in observed retention performance, partic-
31 ularly in temperate climates of the northern hemisphere, where there are
32 distinct seasonal variations in temperature, rainfall patterns, and other cli-

33 matic variables. Retention performance is consistently higher in the warmer
34 summer months of the year (Mentens et al., 2006; Uhl and Schiedt, 2008;
35 Poë et al., 2015; Elliott et al., 2016). This is widely attributed to the in-
36 creased levels of evapotranspiration, resulting in greater recovery of storage
37 capacities between rainfall events. Beyond temperate conditions, however,
38 Voyde et al. (2010) did not observe any seasonal trends in retention perfor-
39 mance for a 12-month study conducted in Auckland, New Zealand, owing to
40 the small seasonal meteorological differences in Auckland’s climate. In the
41 humid-subtropical climate of Hong Kong, Wong and Jim (2014) identified
42 the weakest retention performance in summer months (over a 12-month pe-
43 riod) due to increased levels of rainfall, which prevented sufficient recovery of
44 the green roofs storage capacity between events. Therefore, whilst seasonal
45 variations in observed retention performance are expected and observed in
46 temperate climates, the challenge is to identify whether these variations are
47 wholly due to climate or whether changes also occur in the underlying physi-
48 cal properties that affect the system’s fundamental retention characteristics.

49 Fewer studies have focused on the longer-term (year-on-year) performance
50 evolution of extensive green roof systems. Mentens et al. (2006) and Hill et al.
51 (2016) widely sampled existing green roof systems in Germany and Canada
52 respectively, with both finding no statistical correlation between roof age
53 and hydrological performance. However, no systematic year-on-year com-
54 parisons have been published. Whilst this partly reflects the scarcity of
55 long-term hydrological records, it should also be noted that the effect of nat-
56 ural climatic variation on observed hydrological performance is expected to
57 mask any subtle changes in the underlying hydrological characteristics of the

58 system (De-Ville et al., 2017). Observed retention performance is strongly
59 influenced by storm event characteristics and tends to be greatest for small
60 events, as green roofs only have a finite maximum retention capacity (e.g.
61 20 mm for an extensive system, Stovin et al. (2012)). It is not meaningful to
62 compare annual retention performance (either volumetric or mean per-event
63 retention), as rainfall patterns, temperatures, and other climate variables
64 differ significantly from year-to-year. For example, the same roof configura-
65 tion undergoing a high rainfall-low Antecedent Dry Weather Period (ADWP)
66 year/season/storm event will have a lower retention performance than if ex-
67 posed to a low rainfall-high ADWP year/season/storm event. However, the
68 green roof’s fundamental capacity for retention, as dictated by its physical
69 characteristics, may be the same in both scenarios.

70 Similarly, observations of temporal changes in detention performance are
71 typically confounded by the controlling effects of retention (Wong and Jim,
72 2014; Stovin et al., 2015b), and have therefore rarely been explored in iso-
73 lation. In summary, the literature clearly identifies patterns in sub-annual
74 hydrological performance, whilst findings on longer-term changes to either
75 retention or detention capabilities are inconclusive. No previous studies have
76 attempted to disaggregate storm event or climate-related forcing factors from
77 potential seasonal or longer-term changes to the roof’s underlying hydrolog-
78 ical response.

79 *1.2. Objectives*

80 This study aims to test the null hypothesis that neither sub-annual nor
81 long-term temporal variations exist in the potential hydrological performance
82 of green roof systems that have been monitored in Sheffield, UK. This is to be

83 achieved through: 1) the identification of approaches that permit temporal
84 variations in the physical properties that control retention and detention
85 to be quantified; 2) the exploration of a long-term hydrological record of
86 a series of extensive green roof test beds to identify temporal variations in
87 both potential retention (5-year record) and detention performance (6-year
88 record); and 3) an evaluation of the consequences of any predicted changes
89 through the prediction of hydrological performance in response to design
90 storms.

91 **2. Literature Review**

92 *2.1. Physical controls on potential hydrological performance*

93 A green roof's maximum retention capacity is widely attributed to be
94 approximately equal to the substrate's Plant Available Water (PAW, mm),
95 which is itself a function of the substrate's Field Capacity (Θ_{FC} , %v/v),
96 Permanent Wilting Point (Θ_{PWP} , %v/v), and depth (d , mm):

$$PAW = (\Theta_{FC} - \Theta_{PWP}) \cdot d \quad (1)$$

97 It is proposed that tracking of these physical properties over time should
98 provide a climatically independent temporal evaluation of the Absolute Re-
99 tention Capacity (ARC) of the green roof system (equivalent to the maxi-
100 mum potential soil moisture deficit). These independent ARC evaluations
101 may be combined with the observed effects of rainfall, ADWP, and PET in
102 appropriate hydrological models to identify the Potential Retention Capacity
103 (PRC) and Potential Retention Performance (PRP) of the green roof system
104 in response to a specific climate/weather/storm event scenario. Section 3.3

105 outlines a novel approach to tracking field capacity using in-situ moisture
106 content sensors.

107 As with retention, the system's detention characteristics may also be mon-
108 itored through the identification of relevant physical properties. Detention
109 processes may be modelled via the application of appropriate unsaturated
110 media flow relationships. However, the governing equations for predicting
111 unsaturated-media flow are complex, require numerous physical character-
112 istics (Palla et al., 2012), and there is therefore scope for large compound
113 errors. Alternatively, semi-empirical descriptions of the fundamental deten-
114 tion characteristics can be achieved with simple hydrological models, whilst
115 maintaining suitable levels of predictive accuracy. Stovin et al. (2015a) pro-
116 posed the use of a reservoir routing model to describe detention processes,
117 and this approach was successfully deployed to identify differences in de-
118 tention characteristics between various roof configurations independently of
119 climate.

120 In summary, conventional retention and detention performance metrics
121 derived from monitored data are poorly suited to the identification of tempo-
122 ral trends in underlying hydrological function. It is therefore proposed that a
123 coupled physical property monitoring programme and validated hydrological
124 modelling approach will better identify changes to the underlying green roof
125 physical characteristics and their impacts on potential hydrological perfor-
126 mance over time.

127 *2.2. Temporal trends in green roof physical characteristics*

128 Whilst yearly evaluations of hydrological performance may not exist in the
129 literature, there have been some attempts to characterise temporal changes in

130 green roof physical properties. Exploration of properties thought to directly
131 influence hydrological performance has identified potential for improved hy-
132 drological performance in the long-term. Getter et al. (2007) found that
133 pore volume doubled over a 5-year period, and hypothesised that this would
134 lead to improvements in retention performance due to an increase in micro-
135 porosity ($\leq 50 \mu\text{m}$). However, Getter et al. (2007) also noted that these
136 improvements may come at the expense of worsened detention performance
137 due to an increased presence of macropore ($> 50 \mu\text{m}$) channels. De-Ville
138 et al. (2017) explored the physical properties of virgin and aged (5-years)
139 green roof substrate, where observed structural differences were inferred to
140 lead to improved retention performance with age. Inconclusive results pre-
141 vented the identification of any trends in detention performance, but it was
142 highlighted that — due to the controlling nature of retention performance —
143 overall hydrological performance is likely to remain consistent, if not improve,
144 with increasing system age.

145 In a study of green roof establishment, Emilsson and Rolf (2005) observed
146 a net loss of organic matter (unspecified origin) from 3 to 1% of the total
147 substrate volume over a single year. Bouzouidja et al. (2016) identified similar
148 falls in organic content (1:1 peat dust and pine bark) over a 4 year-period
149 and reported a reduction in the mass of particles smaller than 2 mm in
150 diameter. The impact that organic matter fluctuations can have on green
151 roof hydrological performance is demonstrated by the laboratory experiments
152 of Yio et al. (2013), where a threefold increase in organic content (coir) was
153 associated with a peak attenuation (detention performance) increase from 15
154 to $>50\%$.

155 The changes in physical characteristics noted above will influence the
156 substrate's field capacity and/or its detention response. The present study
157 focuses on the use of long-term hydrological monitoring data from green roof
158 test beds to identify sub-annual (seasonal) and longer-term changes in these
159 underlying system characteristics.

160 **3. Methodology**

161 *3.1. Introduction to the Hadfield Test Beds*

162 The Hadfield Test Beds comprise 9 differently-configured green roof test
163 beds located at the University of Sheffield's Green Roof Centre on a third-
164 floor terrace of the Sir Robert Hadfield Building (Grid Reference 53.3816,
165 -1.4773). Each test bed (TB) configuration has a different substrate compo-
166 sition and vegetation treatment pairing (Figure 1). The test beds are 1 m
167 wide by 3 m long and are installed at a 1.5° slope. Each test bed physically
168 comprises, from base to surface, a hard plastic tray, a drainage layer (ZinCo
169 Floradrain FD 25-E), a filter sheet (ZinCo Systemfilter SF), one of three
170 substrates to a depth of 80 mm, and one of three vegetation treatments.

171 **[Approximate location of Figure 1]**

172 The first two substrates are commercially available substrates manufac-
173 tured by Alumasc ZinCo, Heather with Lavender (HLS) and Sedum Carpet
174 Substrate (SCS). HLS is installed in TB1, TB4 and TB7, with SCS being in-
175 stalled in TB2, TB5 and TB8. The third substrate is a bespoke mix based on
176 Lightweight Expanded Clay Aggregate (LECA) and is installed in TB3, TB6
177 and TB9. HLS is a semi-intensive commercial substrate consisting of crushed
178 brick and pumice (ZincolitPlus), enriched with organic matter including com-

Property	Units	HLS	SCS	LECA
Particle size < 0.063 mm	% (m/m)	2.1±1.4	1.4±0.3	0.4±0.0
Median particle diameter, d_{50}	mm	4.7±0.7	5.2±0.3	5.0±0.1
Dry density	g/cm ³	0.95±0.04	1.06±0.05	0.41±0.00
Wet density	g/cm ³	1.36±0.02	1.45±0.07	0.76±0.02
Total pore volume	% (v/v)	63.8±1.6	59.8±2.0	84.8±0.0
Field Capacity, Θ_{FC}	% (v/v)	41.2±2.3	39.1±2.1	35±1.6
Air content at Θ_{FC}	% (v/v)	22.6±0.8	20.7±4.1	49.8±1.5
Permanent Wilting Point, Θ_{PWP}	% (v/v)	6.6	2.9	2.1
Hydraulic Conductivity, K_{sat}	mm/min	1-15	10-35	≥35
Organic content	% (m/m)	3.8±0.1	2.3±0.5	6.0±0.3

Table 1: Substrate physical characteristics as derived according to FLL (2008) test methods, Mean \pm Standard deviation (Stovin et al., 2015b).

179 post with fibre and clay materials (Zincohum). SCS is a typical extensive
180 green roof substrate consisting of crushed bricks (ZincoLit), enriched with
181 Zincohum. The LECA-based substrate contains LECA as the sole mineral
182 component, with loam and compost. The physical characteristics of these
183 substrates are presented in Table 1.

184 The three vegetation treatments comprise two planted test groups and a
185 single un-vegetated group. TB1, TB2 and TB3 were vegetated with Alumasc
186 Blackdown Sedum Mat, TB4, TB5 and TB6 were vegetated with a Meadow
187 Flower mix, whilst TB7, TB8 and TB9 were unvegetated. The sedum veg-
188 etation was chosen as it is a commonly adopted species for extensive green
189 roof applications due to its tolerance of drought, extreme temperatures and
190 high wind speeds (VanWoert et al., 2005). The Meadow Flower treatment
191 comprises a mix of flowers, grasses and succulents. These species exhibit

192 a lower drought tolerance (Lu et al., 2014) but greatly increase the biodi-
193 versity potential compared to Sedum (Benvenuti, 2014). The unvegetated
194 test bed configurations were created to provide a control against which the
195 contribution of vegetation could be evaluated.

196 Data collected from the Hadfield Test Beds has been previously reported
197 by Berretta et al. (2014) and Stovin et al. (2015a), where the influence of
198 vegetation and substrate characteristics on moisture content behaviour and
199 overall hydrological performance were explored respectively. The findings of
200 Stovin et al. (2015a) are particularly relevant to this study, although only
201 aggregated hydrological performance statistics over their entire 4-year study
202 period were presented.

203 *3.2. Monitoring Study Data Collection*

204 The experimental setup included a Campbell Scientific weather station
205 that recorded hourly wind speed, temperature, solar radiation, relative hu-
206 midity and barometric pressure. Rainfall depth was measured at one minute
207 intervals using three 0.2 mm resolution ARG-100 tipping bucket rain gauges
208 manufactured by Environmental Measures Ltd. The rain gauges were lo-
209 cated at the same height as the test beds, between TB1 and TB2, TB5 and
210 TB6, and beside TB9 (Figure 1). Runoff was measured volumetrically in 25 l
211 collection tanks equipped with Druck Inc. PDCR 1830 pressure transducers.
212 The collection tank located under each test bed was designed for increased
213 measurement sensitivity at the beginning of each rainfall event and to avoid
214 direct discharge onto the sensor. The pressure transducers were calibrated
215 against collected volumes on site. An electronic solenoid valve emptied the
216 tank when maximum capacity was reached (8.3 mm runoff depth) and ev-

217 ery day at 14:00. Runoff was recorded at one minute intervals. Data were
218 recorded using a Campbell Scientific CR3000 data logger.

219 Water content reflectometers were located at three soil depths to measure
220 the soil moisture profile and behaviour in four of the nine test beds (TB1,
221 TB2, TB3 and TB7). The sensors used were Campbell Scientific CS616
222 Water Content Reflectometers. The probes were installed horizontally at
223 the centre of each test bed and the rods were located at 20 mm (bottom),
224 40 mm (mid) and 60 mm (top) above the drainage layer and filter sheet.
225 Considering the proximity of the probes in each test bed, the rods of the mid
226 and top probes were installed at 90° and 180° respectively from the lower
227 one, in order to avoid distortion of the measurement reading taken by the
228 enabled probe. The orientation of each probe was pre-determined to ensure
229 that the wires did not interfere with the accuracy of the measurements from
230 nearby probes. Furthermore, to avoid inter-probe interference, the probes
231 were differentially-enabled, with each of the four sub-scans measuring three
232 probes in different test beds. Moisture content measurements were recorded
233 at 5 min intervals. Moisture probes were calibrated in the laboratory before
234 being installed into the test beds (as described in Berretta et al. (2014)).

235 The Hadfield test beds have been in place since late June 2009. After
236 a commissioning period, rainfall and runoff data collection began in Febru-
237 ary 2010. Climate data were collected from June 2010 and moisture data
238 from January 2011. This study uses data collected from all sources between
239 February 2010 and February 2016. Throughout the monitoring period the
240 runoff collection system experienced some failures. The failures were caused
241 by clogging of the automatic barrel-emptying valves with fine particulate

242 material washed out from the test beds. Even with regular maintenance
243 the collected rainfall/runoff dataset is not complete; this prevents the re-
244 porting of annual volumetric retention metrics and requires the adoption of
245 ‘per-event’ analysis. The 6-year data record is made up of 503 individual
246 rainfall events where total precipitation exceeded 2 mm and the inter-event
247 period exceeded 6-hours. An inter-event period of 6-hours was chosen to al-
248 low comparability with previous studies (Stovin et al., 2012), whilst a 2 mm
249 minimum rainfall depth is considered to be the amount of rainfall typically
250 retained by a non-green roof (Voyde et al., 2010).

251 *3.3. Identifying & Modelling Potential Retention Performance*

252 *3.3.1. Identifying temporal changes in field capacity*

253 The ageing study utilised all three data types collected from the Hadfield
254 beds: climate; rainfall/runoff; and moisture content. Each rainfall event
255 where rainfall (P) and runoff (R) were greater than 2 mm was identified
256 from the 6-year data record (between 98 and 198 events depending on the
257 test bed).

258 As previously outlined, the identification of any year-on-year trends in
259 retention performance using monitored rainfall and runoff data is of limited
260 value due to the dominant effects of climatic factors. Therefore, a physi-
261 cal property monitoring approach was adopted to assess how the *potential*
262 *maximum retention depth* of the green roof varied over time. The moisture
263 content (Θ) of the substrate was monitored continuously using the moisture
264 content probes installed into TB1, TB2, TB3 and TB7. Theoretically, runoff
265 only occurs from a green roof once the substrate has reached field capacity
266 (Θ_{FC}). Therefore, after the point of runoff initiation, the substrate should

267 be at/around Θ_{FC} . Due to the highly permeable nature of green roof sub-
268 strates, any significant saturation above Θ_{FC} is unexpected. The substrate's
269 field capacity was therefore defined as the moisture content of the substrate
270 2 hours after the cessation of rainfall. Only events that generated >2 mm
271 runoff were considered.

272 The observed field capacity values were analysed over two temporal scales,
273 by study-year, and continuously over a Julian year. Categorical evaluations
274 were undertaken statistically using the non-parametric Kruskal-Wallis Test
275 method for identifying significant differences in distribution and to explore
276 the presence of trends over time.

277 Continuous evaluations were undertaken by fitting a Fourier series model
278 to the data to identify sub-annual trends in Θ_{FC} . The Fourier series model
279 takes the form:

$$\Theta_{FC} = a + b \cdot \cos(D \cdot p) + c \cdot \sin(D \cdot p) \quad (2)$$

280 where a , b , and c are optimised parameters, p was set equal to $2\pi/365$, Θ_{FC}
281 is the monitored field capacity and D is day of the year (where January 1st
282 is 1 and December 31st is 365, 366 in a leap year). Model fit was evaluated
283 with the R^2 goodness of fit statistic and a bisquare weighting of residuals.

284 3.3.2. Modelling potential retention performance

285 The identified values of Θ_{FC} allow for temporal evaluations of the maxi-
286 mum retention capacities of the green roof systems. Retention performance,
287 as previously established, depends upon Θ_{FC} , but is also a function of rainfall
288 patterns, ADWP, and PET values. These additional factors can be incor-
289 porated as part of a conceptual hydrological flux model to better identify

290 potential retention performance, whereby:

$$S_{max} = PAW = (\Theta_{FC} - \Theta_{PWP}) \cdot d \quad (3)$$

291 S_{max} is the maximum storage capacity of the substrate in mm, taken here to
 292 be equal to PAW and determined from the difference in Θ_{FC} and the Per-
 293 manent Wilting Point (Θ_{PWP} , Table 1) multiplied by the substrate depth
 294 (d) in mm, 80 mm in this study. S_{max} is used to define the storage through
 295 time (S_t). The stored water depth at time t (S_t , mm) is calculated as the
 296 stored water depth from the previous time step (S_{t-1} , mm) minus the ex-
 297 pected evapotranspiration (ET , mm). Expected ET is estimated by scaling
 298 Potential ET (PET_t , mm) with a moisture limited Soil Moisture Extrac-
 299 tion Function (SMEF) based upon an effective substrate saturation between
 300 Θ_{PWP} and Θ_{FC} (Stovin et al., 2013). PET is calculated using the Hargreaves
 301 method and long-term climate averages for Sheffield, UK (Figure 2).

$$S_t = S_{t-1} - (PET_t \cdot \frac{S_{t-1}}{S_{max}}) \quad (4)$$

302 The Potential Retention Capacity at time t (PRC_t , mm) is defined as the
 303 cumulative losses from the initial storage level, in this study set as S_{max} .

$$PRC_t = S_{max} - S_t \quad (5)$$

304 The Potential Retention Performance (PRP , %) in response to a 1-in-30-
 305 year 1-hour Summer design storm event for Sheffield, UK, was determined
 306 via:

$$PRP = \frac{PRC}{P} \cdot 100 \quad (6)$$

307 where P is total rainfall depth (in this case 30 mm). An Antecedent Dry
 308 Weather Period (ADWP) from 0 to 28-days in duration was investigated to
 309 explore PRP under varying climatic conditions.

310 *3.4. Identifying & Modelling Detention Performance*

311 The same monitored rainfall events used for retention performance evalua-
312 tion were also utilised for identifying detention characteristics. As highlighted
313 above, conventional detention metrics derived from monitored field data (e.g.
314 Peak Delay, Peak Attenuation) are often confounded by the controlling ef-
315 fects of retention. Stovin et al. (2015b) proposed the use of a fitted reservoir
316 routing model to act as a descriptor of the physical detention processes oc-
317 curring within an extensive green roof system. This approach provides a
318 descriptor of detention that is independent of retention and climatic effects.

319 Kasmin et al. (2010) suggested that the detention performance of a green
320 roof test bed could be modelled using reservoir routing concepts, whereby:

$$h_t = h_{t-1} + Qin_t - Qout_t \quad (7)$$

321 in which Qin and $Qout$ represent the flow rates into and out of the substrate
322 layer respectively (mm/min), h represents the depth of water temporarily
323 stored within the substrate (mm), and t represents the discretisation time
324 step. $Qout$ is given by:

$$Qout_t = D_S \cdot h_{t-1}^{D_E} \quad (8)$$

325 in which D_S and D_E are the reservoir routing parameters (scale and expo-
326 nent respectively). For h in mm and $Qout$ in mm/min, D_S has the units
327 $\text{mm}^{(1-D_E)}/\text{min}$, whilst D_E is dimensionless. Note: in previous literature, the
328 scale and exponent of the reservoir routing equation were referred to as k
329 and n respectively; they have been altered in this study to avoid confusion
330 with other physical properties and model parameters.

331 Yio et al. (2013) demonstrated that a model based on a fixed value of
332 D_E was capable of predicting observed runoff profiles with almost no loss of

333 accuracy when compared with a model for which both parameters had been
334 optimised. With a fixed value of $D_E = 2$, values of D_S were optimised for
335 each identified rainfall event by fitting the predicted runoff, in response to
336 net rainfall profiles, to monitored runoff profiles. Model fit was evaluated
337 using the R_t^2 goodness of fit statistic.

338 As with retention, the resultant D_S values were analysed at two temporal
339 scales, categorically by study-year, and continuously over a Julian year. Cat-
340 egorical evaluations were undertaken statistically using the non-parametric
341 Kruskal-Wallis Test for identifying significant differences in distribution and
342 to explore the presence of trends over time. Continuous evaluations were un-
343 dertaken by fitting a Fourier series model to the data to identify sub-annual
344 trends in D_S .

345 *3.5. Predicting Overall Hydrological Performance*

346 Identified retention and detention physical characteristics were combined
347 to predict the runoff of the green roof systems in response to a 1-in-30-
348 year 1-hour Summer design storm event — as per the CIRIA SuDS Manual
349 (Woods Ballard et al., 2015) — for Sheffield, UK, to assess the impact of
350 the identified sub-annual and long-term parameter variations. A net-rainfall
351 profile was generated by subtracting total retention losses (PRC) from the
352 beginning of the rainfall event, and this was then routed using the detention
353 model outlined in Section 3.4 combined with appropriate model parameters.
354 A range of ADWP durations, from 0 to 28-days, was investigated to explore
355 any influence on runoff response.

356 4. Results

357 4.1. Study Period Climate

358 The monthly rainfall depths (Figure 2) highlight the typically high levels
359 of variability associated with a temperate climate. Figure 2 also aids in
360 understanding the difficulty of observing similar rainfall characteristics over
361 time; with the exception of June, almost all other months receive vastly
362 different levels of rainfall from year to year. Cumulative rainfall for the 503
363 identified rainfall events totalled 4224 mm, out of a total recorded 4670 mm,
364 representing 90.5% of all rainfall. Characterisation of storm return periods
365 indicated that the vast majority of storms could be classified as having a
366 return period of less than 2 years (for their respective durations). Only 4 of
367 the 503 events were classified as having a return period in excess of 2 years,
368 as defined by the Flood Estimation Handbook (CEH and NERC, 2008).

369 **[Approximate location of Figure 2]**

370 4.2. Moisture Content

371 Figure 3 presents rainfall, runoff and moisture content data for TB1 for
372 six contrasting rainfall events. The events have been selected to illustrate
373 typical responses in summer and winter conditions. The first four events,
374 09/Jun/14, 27/Jul/13, 10/Feb/13 and 26/Dec/14, all relate to conditions
375 where the substrate was either at, or near to, field capacity at the onset of
376 rainfall. Whilst there is some evidence of temporarily raised moisture content
377 levels around the time of the onset of runoff, the important point is that the
378 moisture content is relatively stable and constant following the initiation
379 of runoff. The plots confirm that the moisture content levels recorded 120

380 minutes after the end of an event provide a good estimate of the effective field
381 capacity during the event. The summer events (upper row) show consistently
382 lower effective field capacity values compared with the winter events (middle
383 row).

384 The final two plots illustrate cases where the moisture content prior to
385 the rainfall event was low, close to the permanent wilting point. Whilst these
386 also demonstrate increasing moisture content in response to the rainfall, the
387 patterns are less consistent. For example, there is a far greater difference
388 between moisture content at different depths in the 25/Aug/11 event com-
389 pared with the first four events, and the top probe appears to be registering
390 rising moisture levels after the event ceased on 08/Aug/14. In both of these
391 cases runoff was measured at very low levels of moisture content. These plots
392 suggest that under conditions of extreme dryness the wetting process is un-
393 even and preferential flow paths may lead to runoff before all the substrate
394 has been wetted to field capacity. There is clearly scope for more detailed
395 research on this topic. However, for the purposes of the present study, this
396 dry condition data has been omitted from calculations of seasonal variations
397 in maximum moisture holding capacity. A systematic approach was adopted
398 for the removal of outliers, in which all monitored field capacities lying below
399 1.5 x the interquartile range of a specific test bed's observed field capacity
400 range were excluded. In practice, this resulted in lower cut-off Θ_{FC} values of
401 28.2, 29.2, 12.9, and 24.9% for TB1, TB2, TB3 and TB7 respectively. For
402 the three brick based substrates there were considerably fewer outlier events
403 than for the LECA test bed: 2 events was omitted from TB1; 4 events from
404 TB2; 7with depth of from TB3; and 3 from TB7. There was some common-

405 ality between rainfall event exclusion between test beds. This small number
406 of excluded events represents only 1-6% of the monitored data, dependent
407 on test bed configuration.

408 **[Approximate location of Figure 3]**

409 *4.3. Retention performance*

410 Figure 4 presents the monitored post runoff event field capacity of TB1,
411 TB2, TB3, and TB7 over the study period. Moisture probe data was not
412 available for the first year of the study, and so a 5-year period is used for
413 the evaluation of any trends in Θ_{FC} over time. The bottom of the substrate
414 consistently exhibits a higher moisture content than either the middle or
415 top. The presence of a vertical moisture profile is exaggerated in the vege-
416 tated test beds (TB1-3) compared with the unvegetated TB7. This suggests
417 that plant and root activity contribute to the development of the vertical pro-
418 file. Comparisons between TB1 (Sedum vegetation) and TB7 (Unvegetated),
419 which share the same substrate, reveal that moisture levels are consistently
420 elevated in TB1 over TB7. Berretta et al. (2014) suggested that this phe-
421 nomenon was due to the moisture retention effects of plants and roots, a
422 result of greater entrained organic content. However, Figure 4 also reveals
423 the presence of a sub-annual cycle in which monitored field capacities were
424 highest in the winter months — vertical dotted lines indicate 1st January
425 of each study year — and lowest in the summer. If differences were solely
426 due to vegetative processes, sub-annual trends would be unexpected in the
427 unvegetated TB7.

428 **[Approximate location of Figure 4]**

429 *4.3.1. Long-term performance evolutions*

430 Categorising the monitored field capacity values by study year (Figure 5)
431 clearly reveals significant differences (Kruskal-Wallis, $p \leq 0.05$) in the distri-
432 butions of monitored field capacity over time for the full depth of TB1 and
433 TB7; TB2 and TB3 show less variation over time. There is spread on all of
434 the distributions, some of which is due to systematic sub-annual variations
435 which will be discussed later. Supplementary Dunn’s pairwise comparisons
436 revealed a significant difference between Year-2 monitored field capacity val-
437 ues and all other years. From Year-3 onward there is no significant statistical
438 difference in the value of monitored field capacity for any test bed.

439 **[Approximate location of Figure 5]**

440 *4.3.2. Sub-annual performance variations*

441 The compiled annual monitored field capacity values of the four test beds
442 fitted with moisture content probes are presented in Figure 6. Whilst scatter
443 in the data is evident, as for Figure 4, there is a visible sinusoidal trend in
444 Θ_{FC} over the year. Fourier series models describe this relationship with an
445 acceptable degree of model fit ($R^2 \geq 0.7$). As previously identified, there is
446 considerably less variation in the moisture levels with depth in the unvege-
447 tated TB7 compared to the same, but vegetated, substrate of TB1. All test
448 beds, and all layers, exhibited a minimum Θ_{FC} in July or August, and a
449 maximum around February. Taking the worst-case (i.e. lowest) value of Θ_{FC}
450 from the top layer of each test bed and applying a substrate-specific constant
451 PWP value (Table 1) suggests that the PAW of brick-based substrate config-
452 urations fluctuates by approximately 5 mm within a year. The LECA-based
453 substrate exhibited a much greater variation of 9.6 mm or 62% (about the

454 mean), which is more than 40 times the long-term change.

455 **[Approximate location of Figure 6]**

456 Figure 7 presents the potential retention capacities of each of the four
457 test bed configurations for varying levels of ADWP. The PRC on any day of
458 the year and for an ADWP of up to 28-days can be identified from each plot.
459 PRC is always greatest for the highest ADWP (28-days) as the regeneration
460 of storage capacity by ET is cumulative. Without a variable PAW and at
461 an infinite ADWP the PRC curves shown in Figure 7 would follow a similar
462 relationship to the PET curve of Figure 2, with lower levels of PRC in the
463 winter months and higher levels in the summer months. The effect of a
464 reduced PAW in the summer months is a corresponding reduction in the level
465 of PRC (*compared to a theoretical maximum*); this reduction is most evident
466 at high levels of ADWP. The greatest levels of PRC for all configurations
467 at the highest ADWPs (≥ 21 -days) can be observed to occur in late spring
468 (May). For low levels of ADWP (≤ 7 -days) in the brick-based substrate
469 configurations (TB1, TB3, & TB7), PRP follows a relationship more similar
470 to that of PET, maintaining the highest levels of PRC in summer months.

471 **[Approximate location of Figure 7]**

472 The reduced levels of PAW in the LECA-based substrate of TB3 com-
473 pared to its brick-based counterparts result in lower overall estimates of PRP.
474 When the greater sub-annual variation in PAW of the LECA-based substrates
475 is also considered, PRP is heavily reduced in the summer months for any
476 ADWP ≥ 3 -days and does not exhibit the same plateau in performance as
477 the brick-based substrates.

478 *4.3.3. Summary*

479 By monitoring Θ_{FC} over a period of five years, it was found that sub-
480 annual variations in maximum potential retention are more significant than
481 those identified year-on-year. From Year-1 to Year-5, the greatest change in
482 Θ_{FC} was 12.6% in the unvegetated HLS test bed (TB7), whilst the greatest
483 sub-annual (seasonal) variation (62%) was observed in the sedum vegetated
484 LECA test bed (TB3). Sub-annual variations were found to be up to 40
485 times greater than long-term evolutions (TB3).

486 *4.4. Detention performance*

487 Figure 8 presents a scatter plot of the fitted detention model parameter
488 D_S over time and highlights considerable variation in the data. Sub-annual
489 trends are less apparent than those seen for the retention analysis. Note:
490 higher values of D_S indicate more rapid runoff and so represent reduced
491 detention performance.

492 *4.4.1. Long-term performance evolutions*

493 The grouping of D_S values by study year reveals the long-term trends
494 in median D_S over time (Figure 9). Vegetated test beds (TB1-6) exhibit
495 little or no change in detention performance (as inferred from D_S values)
496 over the six-year study period when compared to unvegetated systems. The
497 vegetated systems also exhibit reduced interquartile ranges compared to the
498 corresponding unvegetated systems. The unvegetated test beds (TB7-9) ex-
499 perience large variations in the yearly-median value of D_S , with TB9 showing
500 a steady year-on-year increase (+151% Year-1 to Year-6). The unvegetated
501 beds have a statistically significant difference in D_S between Year-1 and Year-

502 6. For all three vegetation treatments, LECA test beds generally exhibit the
503 greatest range of D_S values for each year compared to their brick-based coun-
504 terparts.

505 **[Approximate location of Figure 8]**

506 **[Approximate location of Figure 9]**

507 4.4.2. *Sub-annual performance variations*

508 Figure 10 reveals that there is a sub-annual pattern to detention perfor-
509 mance. The scatter plot highlights significant variation in D_S over the year,
510 making trends more difficult to identify visibly compared with retention. The
511 monthly median values of D_S and the applied Fourier series models reveal
512 the presence of an inverted sub-annual relationship compared with Θ_{FC} , with
513 elevated D_S values (i.e. reduced detention) in summer months. However, par-
514 ticularly for TB1, there is a lack of data during the summer months. This
515 low number of data points is unsurprising as retention performance has been
516 demonstrated to be higher in summer months, preventing the generation of
517 sufficient runoff volumes for detention analysis ($R \geq 2$ mm).

518 The installed vegetation of each configuration plays a significant role in
519 dictating the median annual D_S value (Table 2), with the unvegetated test
520 beds (TB7-9) exhibiting higher annual median values of D_S compared to
521 vegetated configurations. However, for the vegetated test beds the vegetation
522 type (Sedum or Meadow-Flower) does not lead to any clear differences in
523 sub-annual variability.

524 **[Approximate location of Figure 10]**

525 Application of the Fourier series model values of D_S for a *detention perfor-*
526 *mance only* (0-day ADWP) runoff response highlights that the greater values

Test Bed	Model Fit (R^2)	Median D_S	Max. Variation (%)	Peak Attenuation (%)	
				Jan	Jul
1	0.75	0.0073	± 25.6	59.5	47.8
2	0.86	0.0061	± 41.7	68.7	49.18
3	0.79	0.0084	± 44.6	63.2	40.5
4	0.82	0.0070	± 47.1	68.1	45.2
5	0.86	0.0079	± 34.6	60.9	44.2
6	0.86	0.0094	± 36.2	57.3	38.9
7	0.74	0.0139	± 31.5	47.2	29.9
8	0.80	0.0105	± 36.5	54.9	36.0
9	0.65	0.0144	± 15.2	38.6	33.5

Table 2: Summary of detention Fourier series model fit, annual median D_S values, the maximum variation from this median value, and peak attenuation values for a 1-in-30-year design storm with 0-days ADWP.

527 of D_S in summer months lead to a reduced peak attenuation (reduced perfor-
528 mance, see the last two columns of Table 2). The vegetated brick-based test
529 beds (TB1 & TB2) exhibit the smallest levels of peak attenuation variation
530 over the course of the year, whilst the unvegetated brick based configura-
531 tion (TB7) and the vegetated LECA configuration (TB3) both experience
532 significantly greater sub-annual variation in peak attenuation. The greater
533 magnitude of variation in TB3 for detention is also present for retention,
534 suggesting that the LECA-based substrate is more susceptible to sub-annual
535 variations in performance than its brick-based counterparts.

536 *4.4.3. Summary*

537 The fitting of the D_S parameter to observed net rainfall/runoff profiles
538 permits the temporal monitoring of detention processes independently of cli-
539 mate and retention effects. For an unvegetated system, long-term evolutions
540 in detention performance (as inferred from D_S values) are significant, with
541 up to 10 times greater increases than those observed sub-annually (e.g. 151%
542 vs. 15% respectively for TB9). However, vegetated configurations generally
543 exhibit greater sub-annual (seasonal) variation compared with long-term evo-
544 lutions (e.g. 42% vs. 12% respectively for TB2). This, in conjunction with
545 the retention findings, suggests that sub-annual variations are more critical
546 than long-term evolutions.

547 *4.5. Overall hydrological performance*

548 *4.5.1. Long-term performance evolutions*

549 Figure 11 demonstrates the differences in overall performance for two test
550 beds installed with the HLS brick-based substrate (TB1 and TB7) alongside
551 a single test bed with a LECA-based substrate (TB9). The model predic-
552 tions incorporate Year-1 to Year-6 changes in the detention model parameter
553 D_S and also apply the relevant monitored field capacity. For TB1, the small
554 increase in Θ_{FC} and small decrease in D_S result in no clearly observable
555 difference in runoff profile from Year-1 to Year-6 at any ADWP, with peak
556 attenuation decreasing by just 4.2% for a 0-day ADWP. The result of a
557 greater change in Θ_{FC} for TB7 is masked by the considerable difference in
558 Year-1 to Year-6 D_S value, which results in a visually distinct 0-day ADWP
559 runoff response from Year-1 to Year-6, with peak attenuation reducing by
560 30.2%. The LECA substrate of TB9 exhibited the greatest change in D_S

561 value from Year-1 to Year-6 and this results in a 45.2% reduction in peak
562 attenuation. The predicted runoff responses of all 3 test beds confirm the
563 stabilising effect that vegetation can have on long-term hydrological perfor-
564 mance, as previously seen in Figures 5 and 9.

565 **[Approximate location of Figure 11]**

566 *4.5.2. Sub-annual performance variations*

567 The predicted runoff responses shown in Figure 12 represent the mini-
568 mum and maximum detention performances of TB1, TB2, TB3 and TB7,
569 and their associated maximum retention potential at these times. All in-
570 stances of minimum detention performance are during the warmer summer
571 months, whilst the maximum detention performance is seen in the winter
572 months. The differences in D_S are significant and evident in the differences
573 between minimum and maximum D_S 0-day ADWP responses; peak attenu-
574 ation improved by 63.1% for TB3 between August and February.

575 The best runoff responses are always achieved at the 28-day ADWP dura-
576 tion due to the additional retention performance, with a maximum peak at-
577 tenuation of 90.4% for TB1 in July. Under minimum detention performance
578 conditions (summer months) there is considerably more variation between
579 the 0-day and 28-day ADWP responses (56.1%, TB1) than under maximum
580 detention performance (winter months, 15.2%, TB1). This is due to the ele-
581 vated levels of PET in the summer months which permit the faster recovery
582 of retention storage, and thus greater potential retention performance.

583 **[Approximate location of Figure 12]**

584 *4.5.3. Summary*

585 The modelling exercise has clearly demonstrated that retention effects
586 dominate over detention effects, with increased ADWP durations resulting in
587 significantly greater improvements in peak attenuation compared with those
588 due to either sub-annual, or long-term changes in detention characteristics.
589 Similarly, for sub-annual variations, PET rates strongly dictate the levels of
590 achievable performance in the cooler winter months.

591 **5. Discussion**

592 *5.1. Retention*

593 *Long-term performance evolutions*

594 In most cases, the presented data suggest that something occurred late
595 in Year-2/early in Year-3 resulting in increases to field capacity, particularly
596 in the lower substrate layers. Such a clear divide between Year-2 and Year-3
597 could indicate the end of the primary consolidation process of the substrate.
598 Whilst substrate levels were not measured, significant substrate consolidation
599 was not visually observed in Year-3 to Year-6, with substrate levels maintain-
600 ing approximate design depths. Hill et al. (2016) identified that substrate
601 depth was not significantly reduced from *original design depth*, even for sys-
602 tems with up to 17-years of maturation. This observation is consistent with
603 data from Year-3 onwards where field capacity – and inferred consolidation
604 – is not significantly different from year-to-year. Consolidation reduces pore
605 sizes, leading to more pores being capable of holding water against grav-
606 ity, thus improving field capacity (Menon et al., 2015). The HLS and SCS
607 substrates are supplied with compaction factors from the manufacturer of

608 1.25 and 1.12 respectively. FLL characterisation of substrate field capacity
609 is undertaken on compacted substrate samples to replicate established roof
610 conditions. A compaction factor of approximately 1.2 is used, whereby 120
611 mm of substrate is compacted to a 100 mm depth for testing. The similarity
612 of monitored field capacity values (Figure 4) and FLL-derived values (Ta-
613 ble 1) from Year-3 onward could indicate a similar level of compaction in the
614 in-situ substrates to the FLL test samples. This further suggests that prior
615 to Year-3 the in-situ substrates were not fully consolidated.

616 In the upper substrate layers the differences between median monitored
617 field capacity in Year-2 and Year-3 are reduced for vegetated substrate con-
618 figurations compared to lower layers and unvegetated configurations. This
619 suggests that the vegetation is playing a role in moderating substrate con-
620 solidation, an observation that has also been made in bio-filter media (Vi-
621 rahsawmy et al., 2014).

622 Whilst substrate consolidation may have led to the observed increased
623 values of Θ_{FC} , the absolute retention storage capacity of the roof may not
624 have increased as predicted. As Θ_{FC} is measured as a percentage, reducing
625 substrate depths (consolidation) will mean that retention capacity will de-
626 crease if Θ_{FC} is constant. The substrate depths of the Hadfield Test Beds
627 were not monitored over the course of the monitoring programme and so it
628 cannot be definitively said that the identified increases to Θ_{FC} have led to
629 corresponding increases in retention capacities. Assuming the following: con-
630 solidation in line with the manufacturer's recommendations for HLS; PWP
631 values equal to those identified by Poë et al. (2015); an initial substrate depth
632 of 100 mm; a final substrate depth of 80 mm; and utilising the median values

633 of monitored field capacity for TB1, potential retention capacity (PRC) in
634 an unaged TB1 would have been approximately 28 mm compared to 26 mm
635 in an aged TB1. This example highlights the importance of understand-
636 ing the relationships between substrate physical properties and hydrological
637 performance.

638 Ultimately, from the analysis of long-term retention performance, there
639 is evidence of an increase in Θ_{FC} between Year-2 and Year-3, but there is
640 little significant change after this point. If these increases in Θ_{FC} are a result
641 of consolidation, then substrate depths are required to assess changes in the
642 absolute potential retention capacity of the system.

643 *Sub-annual temporal variations*

644 Seasonal trends within the monitored field capacity data closely follow
645 expectations of seasonal vegetation behaviour, with greater foliage extent
646 and higher water use in summer months. However, the presence of seasonal
647 changes also in TB7, which is unvegetated, indicate that this is unlikely to
648 be the sole cause. An alternative hypothesis is that a seasonal variation in
649 the substrate's wetting and drying response — as a result of variable water
650 repellency — is being observed. As a substrate dries, just like an ordinary
651 soil, the organic secretions of roots and soil microorganisms become more
652 concentrated. In doing so, these secretions become increasingly hydropho-
653 bic, actively repelling water (Doerr et al., 2000). During winter months,
654 frequent rainfall events and low levels of ET prohibit the substrate from dry-
655 ing excessively (Berretta et al., 2014), preventing the formation of strongly
656 hydrophobic films on substrate particles. Low levels of hydrophobicity al-
657 low water to adhere to substrate surfaces, increasing the moisture content.

658 Contrastingly, in summer, there are fewer rainfall events and higher tempera-
659 tures, allowing for greater depletion of substrate moisture through ET. These
660 conditions allow for the generation of a hydrophobic environment, such that
661 at the onset of the next rainfall event water is repelled from substrate par-
662 ticles (Doerr et al., 2000). This causes rainfall to leave the green roof more
663 quickly and prevents the ingress of water to smaller pores, resulting in lower
664 substrate moisture levels than may otherwise be theorised.

665 *5.2. Detention*

666 *Annual temporal variations*

667 Conventional detention metrics derived from observed runoff are not inde-
668 pendent of retention effects and are poor descriptors of differences in tempo-
669 ral changes in actual detention processes. The application of a hydrological
670 model to simulate detention processes, and the fitting of its parameters, pro-
671 vides an independent and more descriptive overview of potential variation in
672 detention performance in the long-term. The steady year-on-year increase
673 in the value of D_S observed in the unvegetated test beds implies that the
674 driver of this change is a continuously occurring process. The more consis-
675 tent values of D_S over time for vegetated beds suggest that vegetation helps
676 mitigate against the negative effects of this unidentified process on detention
677 performance. A reduction in detention performance (implied by increased
678 D_S values) is perhaps unexpected, if substrate consolidation is occurring —
679 as hypothesised from monitored field capacity observations — then detention
680 performance may be expected to increase. Consolidation reduces substrate
681 pore sizes, potentially reducing the cross-sectional area for water flow, thus

682 resulting in a reduced hydraulic conductivity and a theorised improved de-
683 tention performance (De-Ville et al., 2017).

684 The steady increases in D_S in the unvegetated beds could indicate the
685 steady decay of the initial organic matter content over time. This loss of
686 organic content has been observed in the literature, with Bouzouidja et al.
687 (2016) observing a net loss of organic matter (peat dust and pine bark) from
688 5.0 to 2.1% v/v over 4 years in a vegetated system. Therefore, greater or-
689 ganic losses may be expected in the unvegetated test beds as no new organic
690 matter is entrained through vegetative processes. The long-term stability of
691 different organic matter types within extensive green roof systems remains
692 largely unexplored. However, the use of partially decomposed organic mat-
693 ter (such as peat, and/or peat dust) in new systems may result in greater
694 decomposition than other sources (Ampim et al., 2010). The unvegetated
695 LECA substrate (TB9) experiences the greatest increase in median D_S over
696 the study period, its compost only organic material may have decayed faster
697 than the compost and fibre mix of HLS and SCS. For the unvegetated LECA
698 substrate (TB9), the trend seen in the first 5 years of the study would sup-
699 port this hypothesis of organic content decay, with detention performance
700 deterioration slowing until a steady level is reached around Year-4 to Year-5.
701 This hypothesis could have been confirmed through the repeated sampling
702 and analysis of substrate samples for organic content. The impact that or-
703 ganic matter changes can have on green roof hydrological performance was
704 demonstrated by Yio et al. (2013), where a threefold reduction in organic
705 content (coir) caused peak attenuation to fall from >50 to 15%.

706 *Sub-annual temporal variations*

707 Seasonal trends in D_S are the result of many co-active processes, the
708 most visible cause being vegetation growth phases, evidenced by the gener-
709 ally reduced variation seen for unvegetated test beds (Table 2). It may have
710 been expected that the Meadow-Flower vegetation (TB4-6) would experience
711 the greatest levels of variation, due to the deciduous nature of many of the
712 species, which greatly reduces vegetation coverage in winter months. How-
713 ever, Sedum vegetated configurations experienced the greatest sub-annual
714 variation for 2 of the 3 substrate types (SCS - TB2, and LECA - TB3, Ta-
715 ble 2). This observation, coupled with the presence of sub-annual variation
716 in unvegetated test beds, indicates the presence of additional drivers of vari-
717 ation.

718 The sub-annual variation in substrate water repellency, hypothesised for
719 the retention analysis, also has the potential to influence detention perfor-
720 mance. The greater substrate moisture during winter months and reduced
721 hydrophobicity/repellency permits the movement of water through the small
722 pore networks of the substrate. This leads to increased travel times and
723 ultimately greater detention performance, whilst in summer, increased hy-
724 drophobicity/repellency prevent water ingress into smaller pores and directs
725 it into preferential flow paths (Doerr et al., 2000), reducing travel times and
726 thereby reducing detention performance. The reduced levels of seasonal vari-
727 ation in the unvegetated test beds are therefore believed to be associated
728 with reduced levels of organic matter and the absence of roots. Without
729 these, the generation of hydrophobic conditions is greatly reduced. Com-
730 bining observations for TB9's year-on-year decline in detention performance

731 — hypothesised to be associated with reducing organic levels — with these
732 seasonal trends, adds additional support to the hypothesis of substrate hy-
733 drophobicity/repellency being the main observable driver of seasonal perfor-
734 mance variation.

735 *5.3. Comparison of long-term evolutions and sub-annual performance varia-* 736 *tions*

737 Whilst long-term evolutions in retention and detention performance were
738 observable for vegetated configurations, they generally resulted in insignifi-
739 cant reductions to overall hydrological performance. This evidence of con-
740 sistent long term potential hydrological performance is reassuring given the
741 increasing deployment of extensive green roof systems globally. However,
742 sub-annual changes in the value of D_S were an order of magnitude higher
743 than long-term evolutions. As discussed previously, TB1 experienced a 4% re-
744 duction in peak attenuation from Year-1 to Year-6, but a 15% reduction from
745 winter to summer. This provides further evidence that sub-annual trends are
746 more important in predicting vegetated green roof hydrological performance
747 than long-term trends. As green roof systems are predominantly vegetated,
748 these findings may be of particular importance to stormwater engineers.

749 The inverse relationships of sub-annual retention and detention perfor-
750 mance, are likely to result in a moderately consistent year-round runoff
751 response. Reduced summer detention performance is negated by typically
752 longer ADWPs (greater retention), and elevated winter detention benefits
753 restricted by low levels of PET (reduced retention). Figure 12 highlights
754 these effects whilst also exploring the role of storm duration and return pe-
755 riod. It is seen that extended storm durations and increased return periods,

756 both synonymous with higher rainfall, result in reduced peak attenuation
757 performance in all cases. This further highlights the finite nature of reten-
758 tion capacities and the importance of ADWP duration for storage recovery.

759 **6. Conclusions**

760 This study has explored the temporal variations in potential hydrological
761 performance of a series of extensive green roof test beds with varying con-
762 figuration. Potential retention performance was identified through a novel
763 approach of substrate moisture content monitoring. Detention performance
764 was identified via descriptive hydrological model parameters. Together, these
765 observations permitted the prediction of overall hydrological response varia-
766 tion at sub-annual and long-term temporal scales.

767 Monitored trends in substrate field capacity over time indicate an overall
768 increase in potential retention performance over the study period. The small
769 improvements in retention performance are likely to be the result of substrate
770 consolidation generating more small substrate pores capable of holding water
771 against gravity. Increased consolidation in the unvegetated test bed indicates
772 that root action helps to stabilise retention performance over time. However,
773 the magnitude of these improvements is exceeded by seasonal performance
774 variations.

775 For detention performance, seasonal variation also proved to be more
776 evident compared with annual trends. The steady year-on-year decline in
777 detention performance for unvegetated test beds, compared to the relatively
778 stable yearly performance of vegetated test beds, suggests that organic mat-
779 ter decay is the likely cause of long-term detention performance deterioration.

780 However, this hypothesis needs to be confirmed with monitoring of organic
781 content evolution.

782 The identified sub-annual trends in retention and detention are hypoth-
783 esised to be a result of temporally variable hydrophobicity/water repellency
784 of the substrate. However, PET is also a controlling factor for potential
785 retention performance. In the warmer summer months, water repellency
786 is increased, limiting the elevated summer potential retention generated by
787 greater PET, and directing flow into preferential flow paths thus reducing
788 detention performance. In the cooler winter months, water repellency is low
789 and so does not restrict potential retention performance which is then lim-
790 ited by low levels of PET. Detention performance is maximised under winter
791 conditions as flow is more uniformly distributed throughout the substrate.

792 All of the above findings may help to explain why a Sedum vegetated
793 green roof with a brick-based substrate has become a global industry stan-
794 dard. This configuration is capable of supporting strong levels of retention
795 and detention, without significant long-term deteriorations in performance.
796 However, what has been highlighted is the need for further understanding of
797 the precise drivers of sub-annual variation. Multiple data sources and meth-
798 ods of analysis suggest that sub-annual water repellency cycles could be the
799 driver, but further research is required.

800 **Acknowledgements**

801 Simon De-Ville was supported by an EPSRC DTA Award (EP/L505055/1).

802 **References**

803 Ampim, P. A. Y., Sloan, J. J., Cabrera, R. I., Harp, D. A., Jaber, F. H.,
804 2010. Green Roof Growing Substrates: Types, Ingredients, Composition
805 and Properties. *J. Environ. Hort* 28 (4), 244–252.

806 Benvenuti, S., 2014. Wildflower green roofs for urban landscaping, ecological
807 sustainability and biodiversity. *Landscape and Urban Planning* 124, 151–
808 161.

809 Berretta, C., Poë, S., Stovin, V., 2014. Moisture content behaviour in ex-
810 tensive green roofs during dry periods: The influence of vegetation and
811 substrate characteristics. *Journal of Hydrology* 511, 374–386.

812 Bouzouidja, R., Rousseau, G., Galzin, V., Claverie, R., Lacroix, D., Séré,
813 G., 2016. Green roof ageing or Isolatic Technosol's pedogenesis? *Journal*
814 *of Soils and Sediments*.

815 CEH, NERC, 2008. *Flood Estimation Handbook*. Institute of Hydrology.

816 De-Ville, S., Menon, M., Jia, X., Reed, G., Stovin, V., 2017. The impact
817 of green roof ageing on substrate characteristics and hydrological perfor-
818 mance. *Journal of Hydrology* 547, 332–344.

819 Doerr, S., Shakesby, R., Walsh, R., 2000. Soil water repellency: its causes,
820 characteristics and hydro-geomorphological significance. *Earth-Science Re-*
821 *views* 51 (1), 33–65.

822 Elliott, R. M., Gibson, R. A., Carson, T. B., Marasco, D. E., Culligan, P. J.,
823 McGillis, W. R., 2016. Green roof seasonal variation: comparison of the

- 824 hydrologic behavior of a thick and a thin extensive system in New York
825 City. *Environmental Research Letters* 11 (7), 074020.
- 826 Emilsson, T., Rolf, K., 2005. Comparison of establishment methods for ex-
827 tensive green roofs in southern Sweden. *Urban Forestry & Urban Greening*
828 3 (2), 103–111.
- 829 FLL, 2008. Guidelines for the Planning , Construction and Maintenance of
830 Green Roofing - Green Roofing Guideline. Forschungsgesellschaft Land-
831 schaftsentwicklung Landschaftsbau (FLL).
- 832 Getter, K. L., Rowe, D. B., Andresen, J. a., 2007. Quantifying the effect of
833 slope on extensive green roof stormwater retention. *Ecological Engineering*
834 31 (4), 225–231.
- 835 Hill, J., Drake, J., Sleep, B., 2016. Comparisons of extensive green roof media
836 in Southern Ontario. *Ecological Engineering* 94, 418–426.
- 837 Kasmin, H., Stovin, V. R., Hathway, E. A., 2010. Towards a generic rainfall-
838 runoff model for green roofs. *Water Science and Technology* 62 (4), 898–
839 905.
- 840 Lu, J., Yuan, J.-g., Yang, J.-z., Yang, Z.-y., 2014. Responses of morphology
841 and drought tolerance of *Sedum lineare* to watering regime in green roof
842 system: A root perspective. *Urban Forestry & Urban Greening* 13 (4),
843 682–688.
- 844 Menon, M., Jia, X., Lair, G., Faraj, P., Bland, A., 2015. Analysing the impact
845 of compaction of soil aggregates using x-ray microtomography and water

- 846 flow simulations. *Soil and Tillage Research* 150 (Supplement C), 147 – 157.
847 URL <http://www.sciencedirect.com/science/article/pii/S0167198715000392>
- 848 Mentens, J., Raes, D., Hermy, M., 2006. Green roofs as a tool for solving the
849 rainwater runoff problem in the urbanized 21st century? *Landscape and*
850 *Urban Planning* 77 (3), 217–226.
- 851 Palla, A., Gnecco, I., Lanza, L. G., 2012. Compared performance of a con-
852 ceptual and a mechanistic hydrologic models of a green roof. *Hydrological*
853 *Processes* 26 (1), 73–84.
- 854 Poë, S., Stovin, V., Berretta, C., 2015. Parameters influencing the regener-
855 ation of a green roof's retention capacity via evapotranspiration. *Journal*
856 *of Hydrology* 523, 356–367.
- 857 Stovin, V., Poë, S., De-Ville, S., Berretta, C., 2015a. The influence of sub-
858 strate and vegetation configuration on green roof hydrological performance.
859 *Ecological Engineering* 85.
- 860 Stovin, V., Po, S., Berretta, C., 2013. A modelling study of long term green
861 roof retention performance. *Journal of Environmental Management* 131,
862 206 – 215.
- 863 Stovin, V., Vesuviano, G., De-Ville, S., 2015b. Defining green roof detention
864 performance. *Urban Water Journal* 9006, 1–15.
- 865 Stovin, V., Vesuviano, G., Kasmin, H., 2012. The hydrological performance
866 of a green roof test bed under UK climatic conditions. *Journal of Hydrology*
867 414-415, 148–161.

- 868 Uhl, M., Schiedt, L., 2008. Green Roof Storm Water Retention Monitoring
869 Results. In: 11th International Conference on Urban Drainage. Edinburgh,
870 Scotland, UK.
- 871 UK METOffice, 2016. Sheffield Cdl climate information - Met Office.
872 URL <http://www.metoffice.gov.uk/public/weather/climate/gcqwzq04e>
- 873 VanWoert, N. D., Rowe, D. B., Andresen, J. A., Rugh, C. L., Xiao, L., 2005.
874 Watering Regime and Green Roof Substrate Design Affect Sedum Plant
875 Growth. *HortScience* 40 (3), 659–664.
- 876 Virahsawmy, H. K., Stewardson, M. J., Vietz, G., Fletcher, T. D., 2014.
877 Factors that affect the hydraulic performance of raingardens: implications
878 for design and maintenance. *Water Science and Technology* 69 (5).
- 879 Voyde, E., Fassman, E., Simcock, R., 2010. Hydrology of an extensive liv-
880 ing roof under sub-tropical climate conditions in Auckland, New Zealand.
881 *Journal of Hydrology* 394 (3-4), 384–395.
- 882 Wong, G. K. L., Jim, C. Y., 2014. Quantitative hydrologic performance of
883 extensive green roof under humid-tropical rainfall regime. *Ecological En-
884 gineering* 70, 366–378.
- 885 Woods Ballard, B., Wilson, Udale-Clarke, H., Illman, S., Scott, T., Ashley,
886 R., Kellagher, R., 2015. Ciria c753: The suds manual. Tech. rep., CIRIA.
- 887 Yio, M. H. N., Stovin, V., Werdin, J., Vesuviano, G., 2013. Experimental
888 analysis of green roof substrate detention characteristics. *Water Science
889 and Technology* 68 (7), 1477–1486.

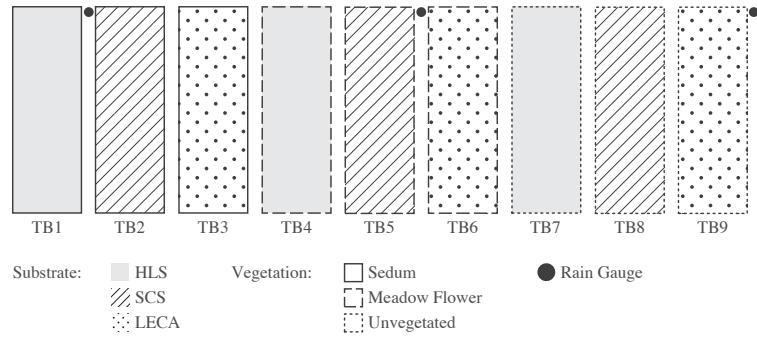


Figure 1: Test bed (TB) configuration layout. The nine test beds are grouped by the three vegetation treatments (indicated by exterior line style) with a repeating substrate order (indicated by shading style). HLS: Heather with Lavender Substrate, SCS: Sedum Carpet Substrate, LECA: Light Expanded Clay Aggregate Substrate. [190x70 mm]

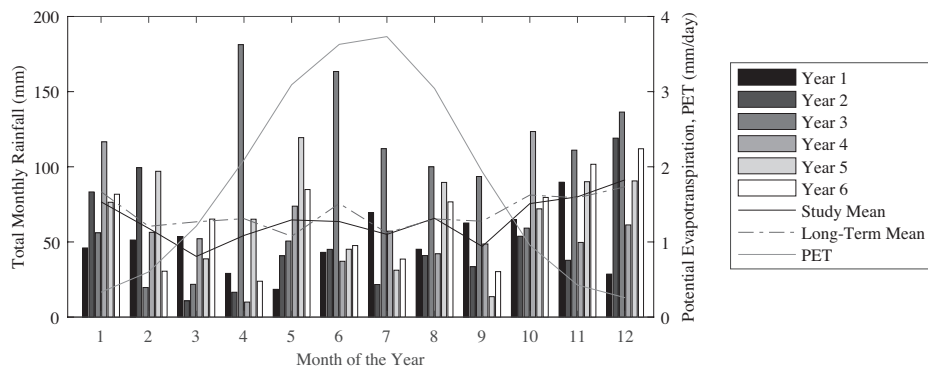


Figure 2: Monthly rainfall data for the 6 year study period compared to the long-term mean (1981-2010) for Sheffield, UK (UK METOffice, 2016), and Hargreaves PET values. [190x70 mm]

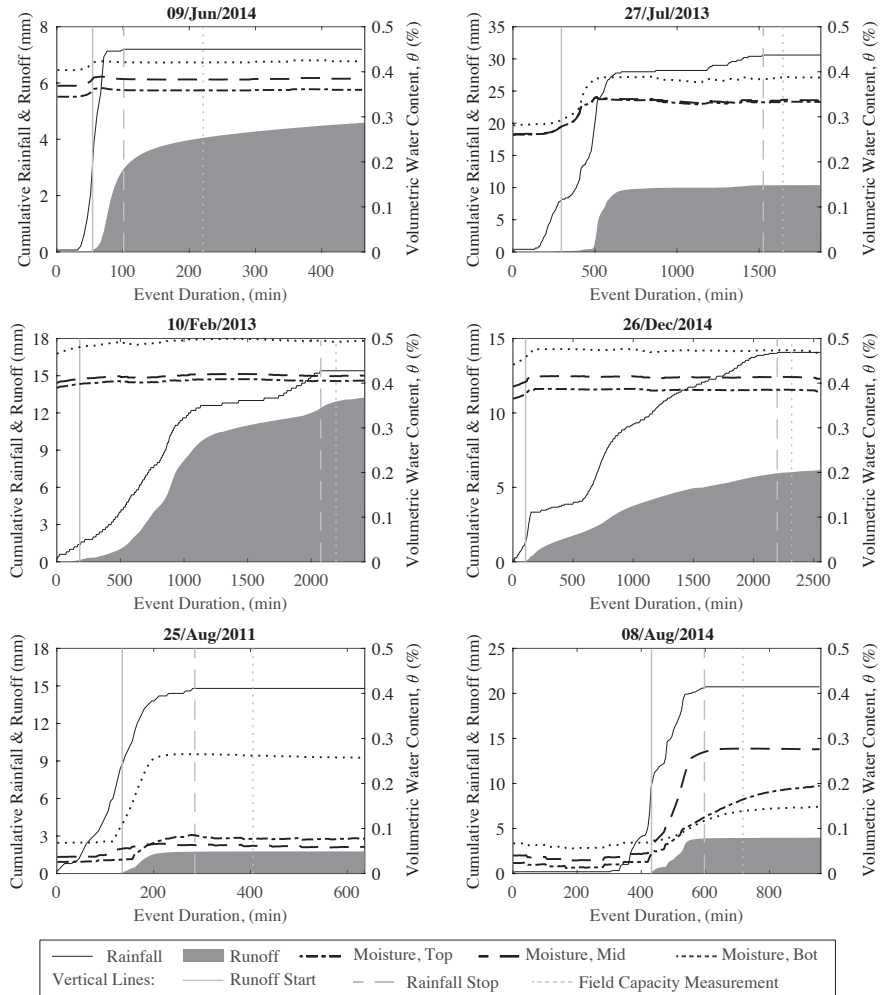


Figure 3: Moisture content profiles for TB1 for various storm events during the study period. [190x190 mm]

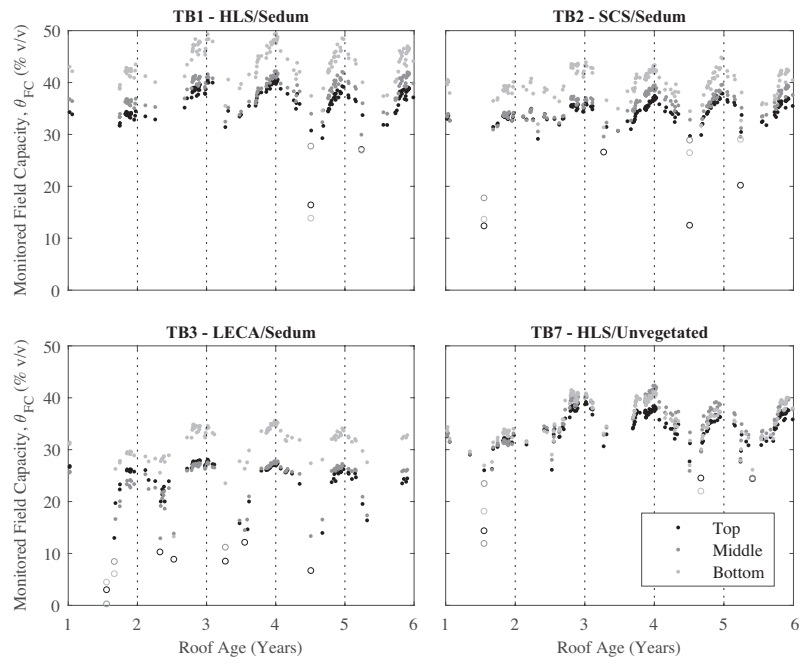


Figure 4: Observed temporal variation in monitored Field Capacity (outlier events included and shown as unfilled circles). [190x140 mm]

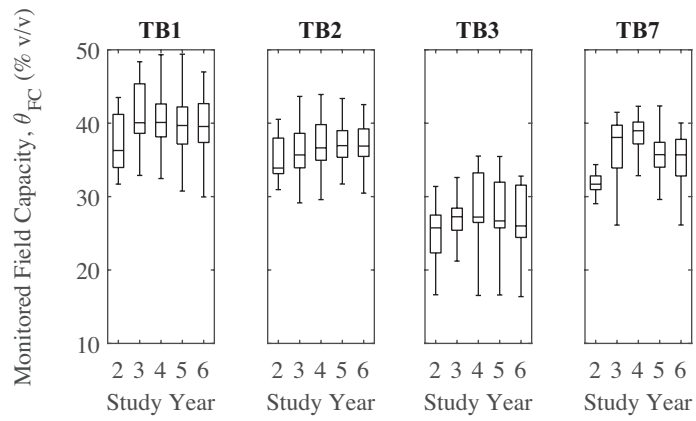


Figure 5: Categorized annual variation in monitored Field Capacity over full substrate depth. [140x60 mm]

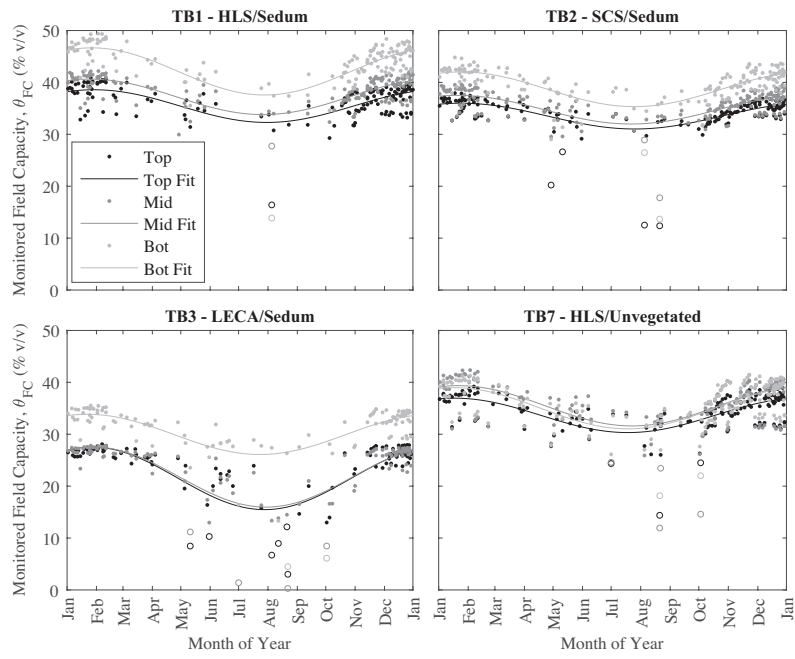


Figure 6: Monitored Θ_{FC} over time including Fourier series model fit (outlier events included and shown as unfilled circles). [190x140 mm]

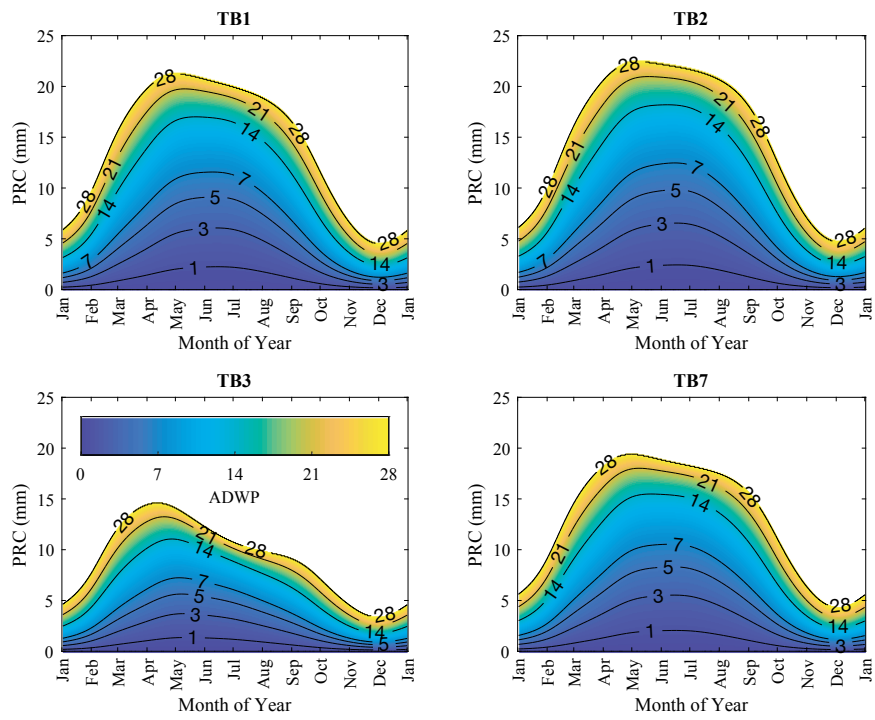


Figure 7: Potential retention capacities (PRC) of the four green roof test beds across a year for varying ADWP durations. Contours indicate ADWP in days.[190x140 mm]

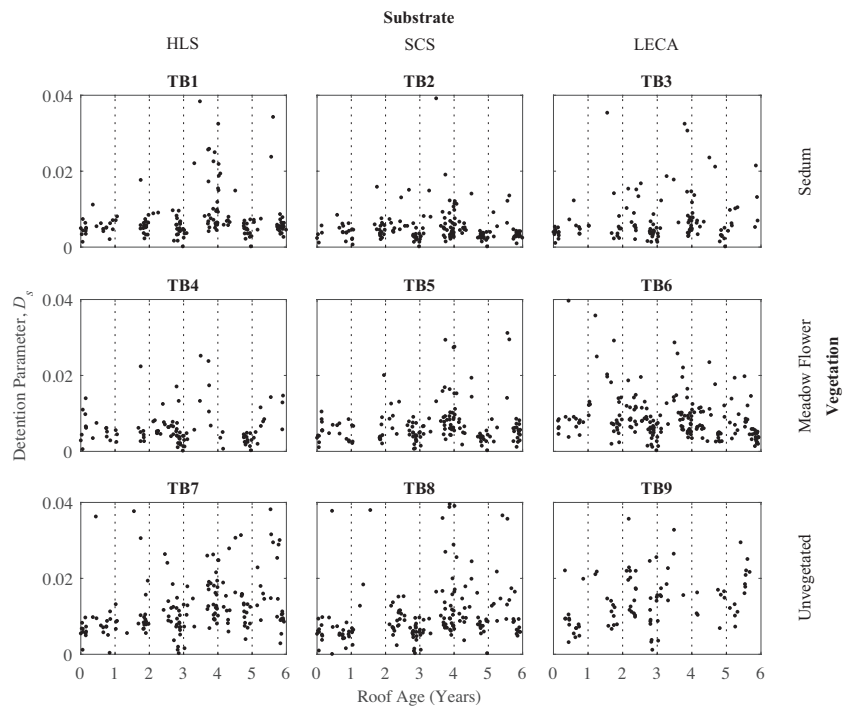


Figure 8: Temporal variation in detention model parameter D_s ($D_s > 0.04$ not shown).
[190x140 mm]

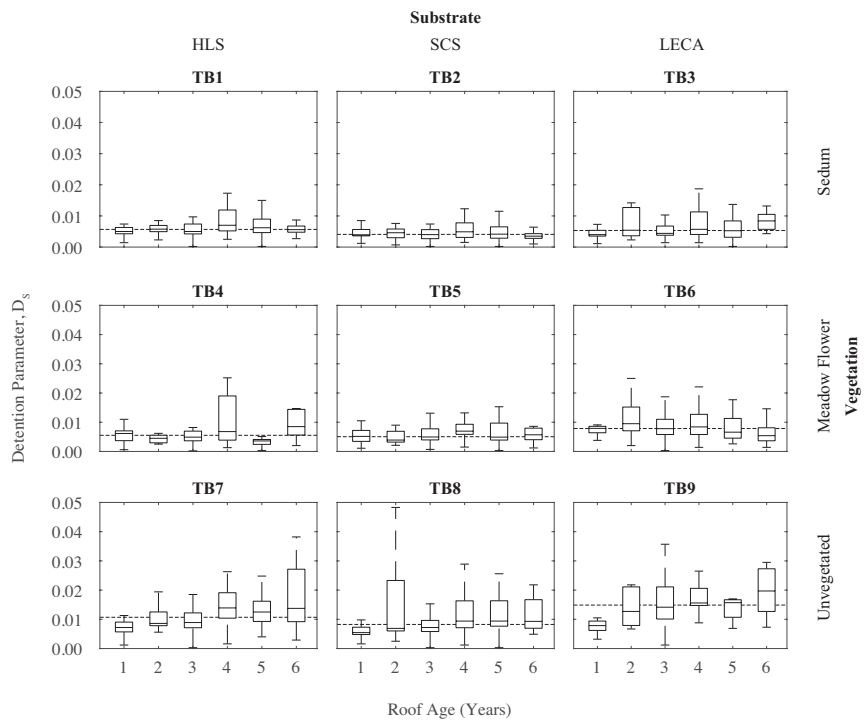


Figure 9: Median values of detention model parameter D_s for each test bed configuration. Dashed horizontal line indicates overall study median. [190x140 mm]

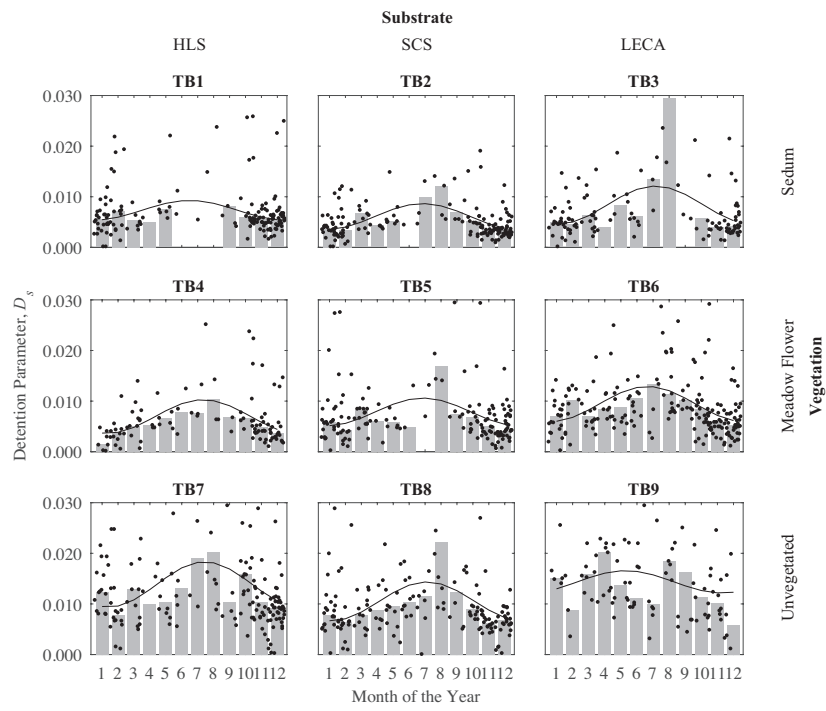


Figure 10: Scatter plot of identified detention model parameter D_S over time including monthly median values (bars) and best fit Fourier series model (line). [190x140 mm]

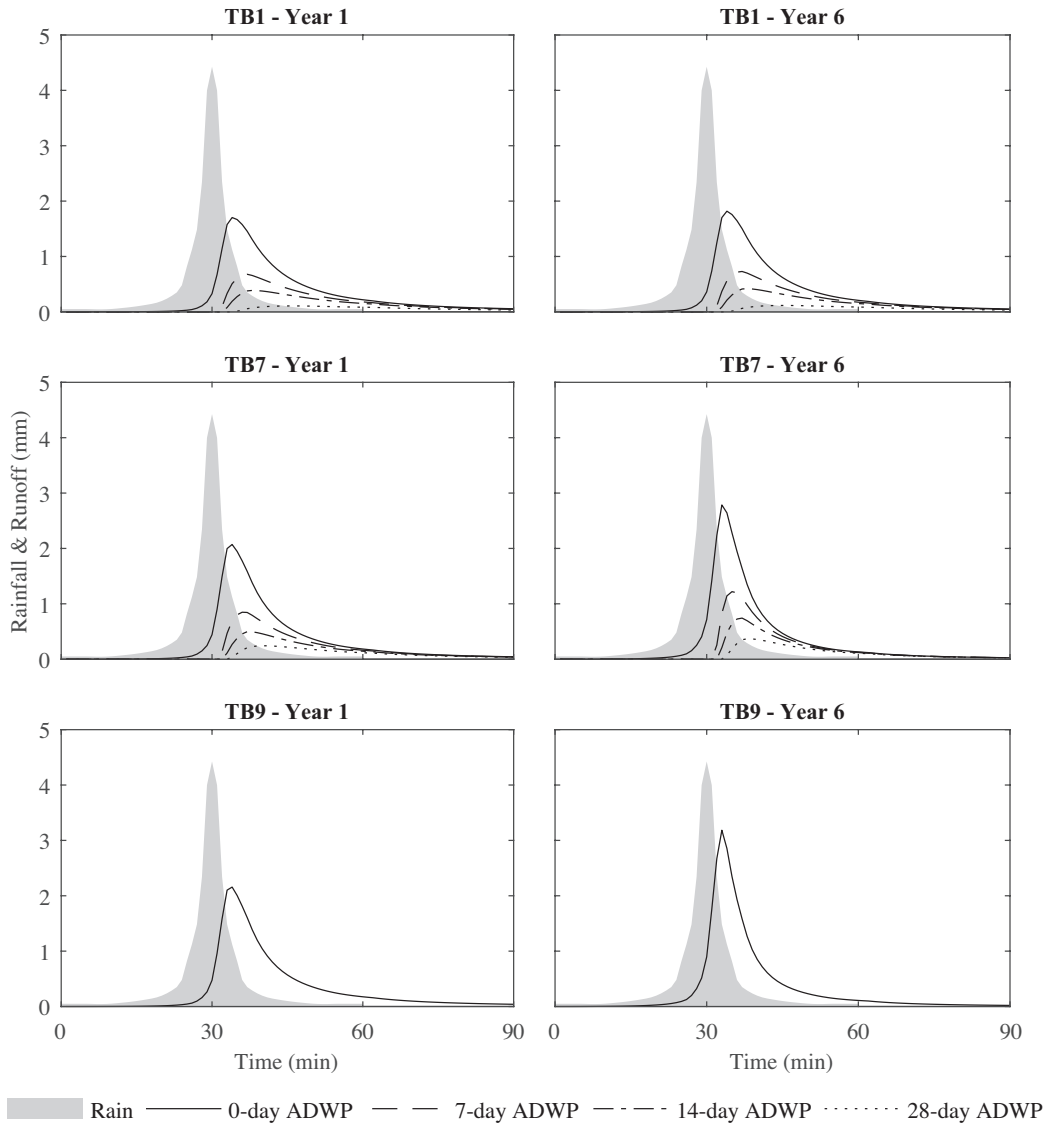


Figure 11: Modelled runoff profiles at Year-1 (left) and Year-6 (right) in response to a 1-in-30-year 1-hour Summer design storm for Sheffield, UK, for varying ADWP. Note: only 0-day ADWP for TB9 as moisture data/retention changes are not available. [190x180 mm]

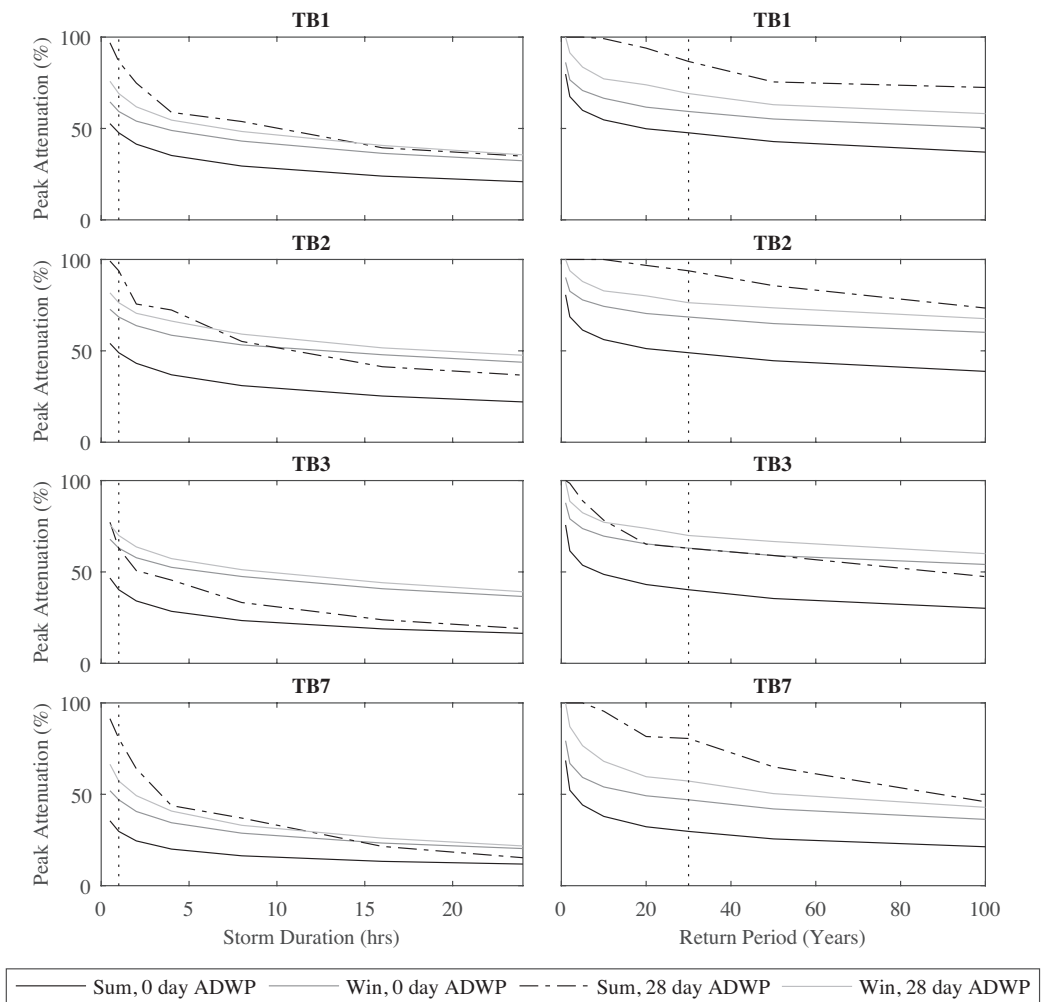


Figure 12: Peak Attenuation values of four test bed configurations for Summer and Winter conditions at 0 and 28-day ADWP durations, with varying Storm Duration (Left) and Storm Return Period (Right). Vertical dashed lines indicate the specific event considered in Figure 11. [190x160 mm]